



Cite this: RSC Adv., 2017, 7, 56220

Comparison between mandibular and femur derived bone marrow stromal cells: osteogenic and angiogenic potentials *in vitro* and bone repairing ability *in vivo*†

Wenhui Zhou,^a Jinkai Zhang,^a Kaili Lin[†] *^b and Fengshan Chen^{*a}

As seed cells for bone tissue engineering, bone marrow stromal cells (BMSCs) have multiple differentiation potential. Prior studies have demonstrated that jaw bone has distinct osteogenic characteristics and different bone repairing capability from limb bone. In order to compare the promotion of bone regeneration as seed cells between maxillofacial derived BMSCs (M-BMSCs) and femur derived BMSCs (F-BMSCs) of SD rats, their proliferation and potential multipotent differentiation abilities, osteogenic differentiation and angiogenic factor secretion were investigated and compared. Moreover, the M-BMSCs and F-BMSCs were seeded on β -tricalcium phosphate bioceramic microspheres, and implanted into alveolar bone crest. The bone regeneration ability induced by the M-BMSCs and F-BMSCs was examined. The results showed that M-BMSCs had better osteogenic capability and angiogenic tendency than those of F-BMSCs both *in vitro* and *in vivo*. M-BMSCs might be the ideal stem seed cell sources for bone regeneration and bone tissue engineering applications.

Received 28th June 2017
 Accepted 8th December 2017

DOI: 10.1039/c7ra07139f
rsc.li/rsc-advances

1 Introduction

Jaw defects are a common clinical manifestation originating from various diseases that will result in facial asymmetry, dysmnesia, and asopia, *etc*. Bone insufficiency is one of the main factors, compromising the prognosis of dental implant surgery, orthodontic and orthognathic treatment. Although human jaw has great potential in regeneration, it is unpractical to expect that a large bone defect can be completely restored spontaneously. Bone tissue engineering, with many advantages in bone repairing over autograft and allograft, is widely used to repair large bone defects and to establish normal functions.^{1–3} The goal of bone tissue engineering is to supply sufficient skeletal dimension through the basis of seed cells, biomaterials and growth factors. As one of the three basic elements of tissue engineering, biomaterials have been extensively investigated for decades,^{4,5} while seed cells, another basic element, serve as the core of tissue engineering and need more attention from researchers.^{6,7}

^aDepartment of Orthodontics, School & Hospital of Stomatology, Tongji University, Shanghai Engineering Research Center of Tooth Restoration and Regeneration, Shanghai 200072, China. E-mail: 13681746901@126.com

^bSchool & Hospital of Stomatology, Tongji University, Shanghai Engineering Research Center of Tooth Restoration and Regeneration, Shanghai 200072, China. E-mail: linkaili@tongji.edu.cn; lklecnu@aliyun.com; Fax: +86-21-66524025; Tel: +86-21-56722215

† Electronic supplementary information (ESI) available: Grows curve of M-BMSCs and F-BMSCs in the 1st generation; average population doubling time. See DOI: 10.1039/c7ra07139f

Among all the seed cells used in clinical application, bone marrow stromal cells (BMSCs) are the ideal seed cells used in bone tissue engineering.^{8–12} They can be easily harvested from the donor bone marrow and have good abilities to form bone tissues *in vivo*. It has been reported that BMSCs isolated from different origins have site-specific cell phenotypic, and contain different functions *in vitro*, especially in maxillofacial. BMSCs from maxillofacial (M-BMSCs) and femur (F-BMSCs) are two important seed cells, which are closely connected and widely used in the clinics as well as the scientific researches. For a long time, although femur flap have been used for inadequate alveolar bone in the palate cleft surgery,^{13,14} the embryological origins between craniofacial and the trunk limb bones are different. Jaw, as the craniofacial bone, arises from neural crest cells of the neuroectoderm germ layer, and undergoes endochondral ossification.¹⁵ While the femur bone, as the axial and appendicular skeleton, arises from the mesoderm, and is formed primarily by intramembranous ossification. The developmental difference contributes to site-specific characteristics and distinct regulation mechanisms between the two cells. During the osteoblastic differentiation and bone formation, these two sources of BMSCs express distinct growth factors, receptors, and signaling pathways.¹⁶

Previous studies have proved that human M-BMSCs isolated from mandibular possess stronger proliferation and osteogenic potential than those of F-BMSCs isolated from long-bone *in vitro*.^{17,18} It might indicate that BMSCs from mandible have unique characteristics and osteogenic capability.¹⁹ During



skeletal development and bone reparation process, the angiogenic capability is pivotal, as the vasculature provides needed nutritive for osteoblast cells and regulates bone remodeling. Moreover, before any blood vessels are detected, the angiogenic factor of VEGF is expressed and this expression has close connection to the early osteogenic process.²⁰ Studies also suggested that human umbilical vein endothelial cells (HUVECs) were allowed to form more sprouting angiogenesis in the co-culture system with craniofacial BMSCs instead of iliac crest BMSCs.²¹ It reveals that M-BMSCs might contain greater angiogenic potency than that of F-BMSCs.

Although the site-specific differences, such as origin, proliferation, and osteogenesis of the two cells have been indicated through different ways, few studies have systematically compared the osteogenic and angiogenic capability between M-BMSCs and F-BMSCs *in vitro* and *in vivo*. Considering that vascularization and bone formation are synchronized sequences through bone defect repairing, we hypothesize that the M-BMSCs possess better abilities for bone formation, which might be due to their better osteogenic and angiogenic capacities. To confirm this, we investigated the differences of osteogenic and angiogenic potential between M-BMSCs and F-BMSCs in the same osteoinductive culture media *in vitro* in the present study. Furthermore, we took β -tricalcium phosphate (β -Ca₃(PO₄)₂, β -TCP) microspheres as biomaterials to load BMSCs, and compared their bone regeneration abilities as the seed cells *in vivo*.

2 Materials and methods

2.1 Isolation and culture *in vitro*

The two week old Sprague-Dawley (SD) rats were purchased from the SLAC Laboratory Animal Co. Ltd (Shanghai, China). All the animal experiments were performed in accordance with the guidelines and regulations for the care and use of laboratory animals of the National Institutes of Health. All procedures were approved by the Institutional Animal Care and Use Committee of Tongji University (Shanghai, China). Rats were sacrificed by cervical dislocation. To collect the M-BMSCs, we removed the soft tissue and periosteum from maxilla, and extracted the third molar. Then we flushed the bone marrow from the superior alveolar ridge, and collected it in the 6 cm cell culture dish with a complete α -MEM (Hyclone, USA) culture medium containing 1% penicillin/streptomycin (Hyclone, USA) and 10% (v/v) fetal bovine serum (FBS, Hyclone, Australia). The F-BMSCs were collected from the same animals.^{18,22} Cells were maintained at 37 °C in a humidified atmosphere of 5% CO₂. Then they were allowed to plate for 3 days. After adherent cells reaching to 80–90% confluence, cells were trypsinised by 0.05% Trypsin-EDTA (1X) (Invitrogen, USA), counted and plated at 3 × 10⁵ cells per cm². The culture medium was replaced every 48 h. The morphological characteristics of BMSCs were observed under inverted microscope for three generations.

2.1.1 Flow cytometric analysis. Cells were collected and washed off with phosphate buffered saline (PBS, Hyclone, Australia). The contents were pipetted to help disperse doublets. Then the cells were resuspended to a concentration of

1 × 10⁷ cells per mL. 100 μ L of the contents were incubated for 45 min on ice with the fluorescently conjugated antibodies (BD Biosciences, USA). Then cells were washed twice and resuspend with PBS. Stained cell samples were analyzed by flow cytometry.²³ The expression of relative surface antigens was then measured through quantitative real time polymerase chain reactions (qRT-PCR) analysis.

2.1.2 Proliferation assay. Cell proliferation assays were performed using the Cell Counting Kit-8 (Beyotime, China). Different generations of the two BMSCs were counted and plated at 2 × 10⁴ cells per well in 96-well plates. Cells were incubated for 6, 12, 24, 48, 72 and 96 h. The culture medium was replaced every two days. The cells number was measured in a microplate reader (SpectraMax M5, Molecular Devices) at 450 nm of reduced WST-8.²⁴ F-BMSCs and M-BMSCs were counted and plated at 5 × 10⁴ cells per well in 24-well plates. Cells were incubated for 6, 12, 24, 48, 72 and 96 h. The cells number was counted, and the population doubling time (PDT) was calculated using the equation: $T \times \log 2 / (\log N_t - \log N_0)$ (N : cell number, T : incubation time 0– t , t : time t , and 0: initial time).²⁵ All experiments were performed in triplicate.

2.2 Osteoblast differentiation assays

The 3rd generation of isolated BMSCs from maxillofacial and femur bones were counted and plated at 3 × 10⁴ cells per cm² in 6-well plates, then cultured in complete osteogenic differentiation medium (Cyagen Biosciences, China) for 14 days. The culture was replaced every three days. All experiments below were performed in triplicate.

2.2.1 Alkaline phosphatase (ALP) activity assay. ALP activity was measured by an alkaline phosphatase assay kit (Beyotime, China). Cells were incubated in osteogenic induction for 3, 7, 10 and 14 days. After being harvested by trypsinization, cells were lysed with 200 μ L of RIPA lysis buffer (Beyotime, China). The total protein content was detected through the BCA protein assay kit (Biotechwell, China). Then, 2.5 μ L of lysate were mixed with 47.5 μ L dilution buffer and 50 μ L of *para*-nitrophenyl phosphate (pNPP), and the mixture were incubated at 37 °C for 10 min. Then the reaction was stopped by adding 100 μ L of the stop buffer. We measured the final absorbance in a microplate reader (SpectraMax M5, Molecular Devices) at 405 nm, and compared it with gradient *p*-nitrophenol as a standard. ALP activity was calculated and normalized to the level of the total protein according to the instructions given in the kit.^{26,27}

2.2.2 Alkaline phosphatase (ALP) staining. Detection of ALP was performed using the alkaline phosphatase detection kit (SiDanSai, China). Cells were incubated in osteogenic induction for 3, 7 and 10 days. Then they were fixed in 10% paraformaldehyde for 2 min, and then washed 3 times with PBS and 2 times with Tris buffered saline tween (e.g. TBST: 20 mM Tris-HCl, 0.15 M NaCl, 0.05% Tween-20). BMSCs were stained by the ALP staining solution for 20 min from light, the color development was stopped by PBS. Then the images were taken through stereoscopic microscope (Leica M205FA, Germany).²⁸

2.2.3 Alizarin Red staining. After 14 days of osteogenic induction, the adherent cells were fixed in 10%



paraformaldehyde for 30 min, then the medium was washed with PBS. Alizarin Red staining (Cyagen Biosciences, China) was used for measuring the calcified tissue in cultures.²⁹ In order to quantify the Alizarin red staining, 10% of cetylpyridinium-chloridemonohydrate was added into each well of the 6-well plate and incubated for 15 min with shaking. The sample were added to 96-well plate and measured in a microplate reader (SpectraMax M5, Molecular Devices).

2.2.4 Quantitative real time polymerase chain reactions (qRT-PCR) analysis. Total cellular RNA was isolated after osteogenic induct for 3, 7, and 14 days. At each time point, the cells were washed twice with PBS, and the RNA was extracted using Trizol reagent (Takara Bio, Japan). The RNA was separated with chloroform and precipitated by adding isopropanol. 70% ethanol in RNase inhibitor diethyl pyrocarbonate (DEPC, Sigma) was added to wash the RNA precipitate twice and the RNA was finally solubilized in the DEPC water. Then the Prime-Script RT reagent kit (Takara Bio, Japan) was used for synthesizing complementary DNA (cDNA) according to manufacturer's recommendations. Primers for amplification of rat alkaline phosphatase (ALP), runt related transcription factor 2 (Runx2), Fibroblast growth factor (FGF2), Transforming growth factor beta1 (TGF β 1), Insulin-like growth factors II (IGF2), Osteocalcin (OCN), Vascular endothelial growth factor (VEGF), Kinase insert domain receptor (KDR), and the housekeeping gene GAPDH were commercially synthesized (Sangon Biotech, China). The primer sequences used for real-time PCR were shown in Table 1. The amplification program was performed through SYBR Premix Ex Taq II (Takara Bio, Japan) as the manufacturer recommended.³⁰ The data was estimated through the $2^{-\Delta\Delta C_t}$ method.

2.2.5 Western blotting analysis. After osteogenic induction is conducted for 7 and 14 days, BMSCs were collected with lysis buffer for western containing phenylmethanesulfonyl fluoride (PMSF) (Beyotime, China). Equal amounts of protein samples

were separated on SDS-PAGE gels and transferred to polyvinylidene difluoride (PVDF) membranes (Beyotime, China). The membranes were blocked with skimmed milk and incubated with rabbit anti-rat ALP, VEGF (Abcam, USA). Then the membranes were washed three times with PBST (PBS containing 0.1% Tween-20 detergent) and incubated with secondary antibodies (Abcam, USA) for 1 h. Finally, the protein bands were detected through BeyoECL Star (Beyotime, China) and exposed them to the analyzer (ImageQuant LAS 4000 mini, GE Healthcare, Sweden).

2.3 Tube formation assay

In order to compare the angiogenic potential between the two kinds of BMSCs, Rat Brain Microvascular Endothelial Cells lines (BMECs) were cultured in the conditioned media from M-BMSCs and F-BMSCs for 3 days. Geltrex™ basement membrane matrix (BD Biosciences, USA) was added to a 24-well plate (300 μ L per well) and incubated at 37 °C for 1 h, then BMECs were seeded onto the layer of Geltrex™ matrix and incubated at 37 °C for 12 h. Three random selected fields of view were captured and the length of tube-like structures was measured.²¹ In addition, the VRGF, KDR, and hypoxia-inducible factor (HIF) gene expression was analyzed by qRT-PCR. The primer sequences used for real-time PCR were shown in Table 1.

2.4 Adipogenic differentiation assays

In order to compare the multipotent differentiation abilities of the two BMSCs, the adipogenic differentiation assay was performed along with the osteogenic differentiation assays. For adipogenic induction, the 3rd generation of isolated BMSCs from maxillofacial and femur bones were counted and plated at 3×10^4 cells per cm^2 in 24-well plates. When cells were confluent, adipogenic differentiation medium (Cyagen Biosciences, China) was used for three cycles of adipogenic treatments. Each consisted of 72 h incubation with adipogenic induction medium (stimulatory supplements including dexamethasone, indometacin 3-isobutyl-1-methylxanthine and insulin) and 24 h incubation with maintenance medium (stimulatory supplements including insulin). Then cells were fixed and stained with Oil Red O. The experiments were performed in triplicate.

2.5 Fabrication of β -TCP microspheres

In the present study, the bioceramics of β -tricalcium phosphate (β -Ca₃(PO₄)₂, β -TCP) microspheres with 120–150 μ m were used as the bone grafts for maxillary defect repairing. The β -TCP microspheres were fabricated according to our previous study. Briefly, the chemical precipitated β -TCP powders after being calcined at 800 °C for 2 h were used as the raw materials to fabricate the β -TCP microspheres *via* the spray-drying method on a high-speed centrifugal spray-drying machine (LGZ-8, Wuxi Dongsheng, China). The spray-dried β -TCP granules were collected and calcined at 900 °C for 3 h, and then cooled to room temperature in the furnace. Finally, the products were sieved to obtain the β -TCP microspheres with 100–120 mesh.^{31,32}

Table 1 Primer sequences for RT-PCR analysis

Gene	GenBank accession number	Primer sequence (5'-3')
ALP	NM_013059.1	5-ACAATGAGATGCGCCAGAG-3 5-CATGTACTTCCGGCCACCA-3
Runx2	NM_053470.2	5-TTCGTCAGCGTCTATCAGTT-3 5-CTTCCATCAGCGTCAACACC-3
FGF2	NM_019305.2	5-GGCTCTACTGCAAGAACGGC-3 5-TAGTTGACGTGTGGTCGCG-3
TGF β 1	NM_021578.2	5-CAGAACCCCCATTGCTGTCC-3 5-AAGACAGCCACTCAGGCGTA-3
IGF2	NM_001190162.1	5-AGTTTGCTGTTCGGACCGC-3 5-GGAAGTACGGCTTGAGAGGT-3
OCN	NM_013414.1	5-AACAATGGACTTGGAGCCCC-3 5-GAAGCCAATGTGGTCGCTA-3
VEGF	NM_031836.3	5-ACGAAAGCGCAAGAAATCCC-3 5-CGGAGTCTGTGTTTGCA-3
KDR	NM_013062.1	5-GCCAGCTCAGGTTTGAGA-3 5-CATGCCCTTAGCCACTTGGGA-3
HIF	NM_024359.1	5-GCAATTCTCCAAGCCTCCG-3 5-ATCAGTGGTGGCAGTTGCG-3



2.6 Animal models

Forty female SD rats (body weight: 200 ± 10 g, age: approximately 8 weeks old, $n = 40$) were purchased from the SLAC Laboratory Animal Co. Ltd (Shanghai, China). Rats were randomly separated into four groups ($n = 10$ in each group): blank control (group B), β -TCP microspheres only (group T), β -TCP microspheres seeded with F-BMSCs (group F), and β -TCP microspheres seeded with M-BMSCs (group M). For each rat in the study group and the control group, the first left maxillary molar was extracted with a dental explorer under pentobarbital-induced general anesthesia, the removal defects were expanded to a uniform size ($2 \times 2 \times 2.5$ mm). For group B, the defect was directly sutured after debridement. For group T, the defect was filled with the β -TCP microspheres. For group F and group M, F-BMSCs and M-BMSCs seeded β -TCP microspheres were implanted into the defect respectively after co-culturing with BMSCs for 12 h. After surgery, rats were housed on a 12 h light/dark cycle with temperature of 25 °C maintained. In each group, 3 SD rats were randomly selected and used for μ CT assay, and the other 3 rats were used for HE staining and immunohistochemistry assay. The rest rats were kept in case of sample damaging. While there was no sample lost or damaged in our study.

2.6.1 Microcomputed tomography analysis. The μ CT system (Scanco Medical, Zurich, Switzerland) was used to track the bone mineral density (BMD) of the newly formed bone tissues after 8 weeks of surgery.³³

2.6.2 Hematoxylin and eosin (HE) staining. Maxillary bones were harvested at week 8 after surgery for histologic analysis. Samples were decalcified and embedded into paraffin. Then the HE dyeing was used to the deparaffined sections. The results were observed under a light microscope (Olympus BX51, Japan), and the percentage of the new bone area was quantified through a personal-computer-based image analysis system (Image-Pro plus 6.0, Media Cybernetic, USA). All experiments were performed in triplicate.

2.6.3 Immunohistochemistry. Rabbit anti-rat ALP and VEGF (Abcam, USA) were performed for the immunostaining procedure on sections. The level of them was analyzed three times through the quantitative integrated optical density (IOD) analysis, and the microscopic regions were selected randomly. The data represented the mean of three quantifications.

2.7 Statistical analysis

The significance of differences was evaluated with a chi-square test using SPSS 20.0 software (IBM, USA). Difference of statistical data was considered significantly at a p -value < 0.05 ($p < 0.05$).

3 Results

3.1 Morphology and flow cytometric analysis

Both of the two BMSCs isolated bone marrow stromal cells showed typical spindle-like fibroblastic morphology, and grew as helix in shape. F-BMSCs appeared aging at the 6th generation, while M-BMSCs appeared no remarkable morphological changes (Fig. 1a).

From flow cytometric analysis and the real time polymerase chain reactions (qRT-PCR) analysis (Fig. 1c and d), both M-BMSCs and F-BMSCs were positive for CD29 and CD90, while negative for CD45 and CD34. These antibodies were routinely used for characterizing the mesenchymal stem cells and the surface antigens, which did not change after removal of cells from the substrate by trypsin.

3.2 Cell proliferation

CCK-8 assay was used for comparing the cell proliferation behaviors between M-BMSCs and F-BMSCs in this study at different generations. The OD value of M-BMSCs and F-BMSCs increased apparently with the increase of the culture time. In the 1st generation group, the proliferation rate of M-BMSCs showed much higher OD value than that of F-BMSCs through the entire culture period ($p < 0.05$), and the difference got bigger with the increase of the culture time. As for the 6th generation group, the proliferation rate was lower comparing to the 1st generation group (Fig. 1b). In addition, cell number in the 1st generation was counted (Fig. S1†). The results showed that cells entered exponential phase of growth after 24 h of culture, and then entered stationary phase after 72 h of culture. The calculated population doubling time (PDT) for M-BMSCs and M-BMSCs was 41.3 ± 3.2 h and 47.6 ± 4.5 h, respectively. The results indicated higher proliferation rate in M-BMSCs group (Table S1†).

3.3 Multipotent differentiation assays

ALP was the early marker of osteogenic differentiation. In order to compare the osteogenic differentiation, F-BMSCs and M-BMSCs were cultured in osteogenic media for days 3, 7, 10 and 14. ALP staining was stronger in M-BMSCs than that in F-BMSCs at each point in time (Fig. 2a). In addition, the ALP activity also indicated that the ALP expression increased with the increase of the culture time, and peaked at day 10 (Fig. 2b). The expression of ALP activity was at a higher level in M-BMSCs than that in F-BMSCs throughout the osteoinductive process *in vitro*. Alizarin Red staining was further used for observing the mineral deposition of the cultured osteoblasts, and the results showed significant mineral nodes in M-BMSCs compared to F-BMSCs at day 14. The OD value also revealed higher osteogenic capability in M-BMSCs group in qualification (Fig. 2c).

Under the adipogenic conditions, accumulated lipid droplets appeared in F-BMSC group, whereas M-BMSC group contained less adipocytes (Fig. 2d).

3.4 Osteogenic and angiogenic differentiation *in vitro*

The qRT-PCR was used to examine the expression of bone-related genes such as ALP, Runx2, FGF2, TGF β 1, IGF2 and OCN, and angiogenic factors, such as VEGF and KDR on days 3, 7 and 14 (Fig. 3a). The gene expression of ALP and OCN increased apparently with the increase of culture time both in F-BMSCs and M-BMSCs groups. As for Runx2 in M-BMSCs group, with the increase of the culture time from day 3 to day 7, the expression level increased apparently, and then increased slightly with further increasing the culture time to day 14. While



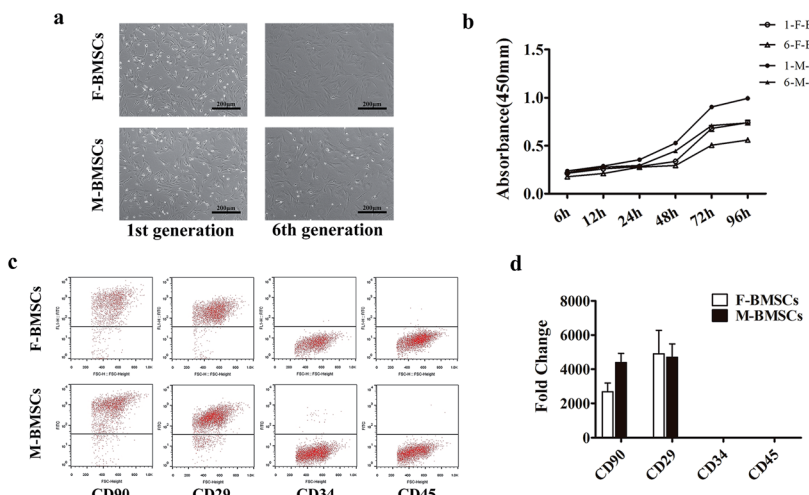


Fig. 1 (a) Morphology of F-BMSCs and M-BMSCs in the 1st generation and 6th generation. (b) CCK-8 assay for cell proliferation. (c) Flow cytometric analysis. (d) The gene expression of the surface markers.

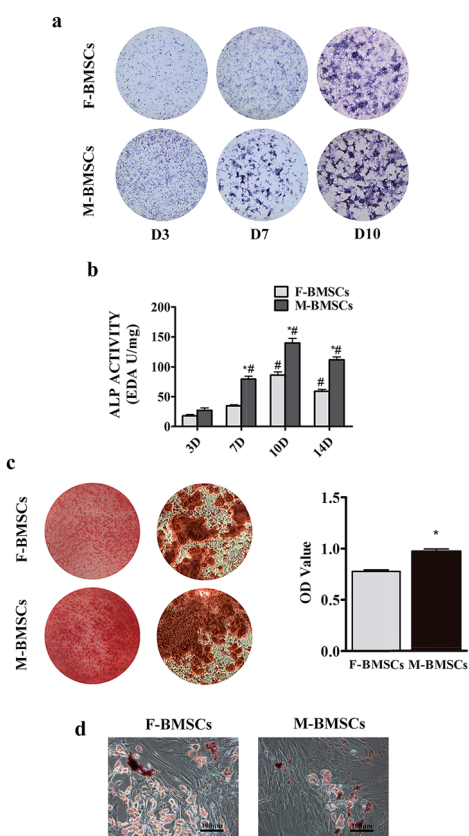


Fig. 2 Multipotent differentiation assays: (a) ALP staining, (b) ALP activity, (c) Alizarin red staining (d) Oil Red O staining. * $p < 0.05$ indicates statistical significance between the M-BMSCs group and the F-BMSCs group; # $p < 0.05$ indicates the statistical significance between day 3 and the other time points in each group.

the Runx2 in F-BMSCs group decreased throughout the culture time. For FGF2, the gene expression decreased with the increase of the culture time in M-BMSCs group, while reached to highest in D7 in F-BMSCs group. For IGF2, M-BMSCs group had higher

gene expression than that of F-BMSCs group in D3 and D14, while in D7, the gene expression was higher in F-BMSCs group. The expression of TGF β 1 was higher in M-BMSCs group in each time point. As for the angiogenesis-related genes, the expression of VEGF in M-BMSCs group decreased with the increase of the culture time. Comparing with F-BMSCs group, M-BMSCs group had higher VEGF expression. Moreover, KDR had relatively higher expression in M-BMSCs group while F-BMSCs group barely expressed this gene. Most importantly, both the osteogenic gene and angiogenic factor expression levels in the M-BMSCs group were significantly higher than those in the F-BMSCs group except the OCN at day 14 and VEGF at day 7.

In order to measure the osteogenic and angiogenic protein expression levels, western blotting analysis was further used to determine the ALP and VEGF protein expression levels on days 7 and 14 (Fig. 3b). The results revealed that gray-scale values of ALP and VEGF for M-BMSCs group were higher than those for F-BMSCs group at each time point.

The angiogenic potential of the two BMSCs *in vitro* was further confirmed by co-cultured with rat brain microvascular endothelial cells (Fig. 4a). After 3 days of supernatant treatment from M-BMSCs (M + MEC group) and the F-BMSCs (F + MEC group), tube-like structures were evident, and the total tube length was significantly increased in the M + MEC group compared with F + MEC group. From the qRT-PCR assay, M-BMSCs contained higher angiogenic gene expression (Fig. 4b).

3.5 Characterizations of β -TCP microspheres

The SEM micrograph result showed that the samples were sphere-like shape (Fig. 5a). The XRD analysis revealed that microspheres were composed of higher crystalline and no second phase other than β -TCP (Fig. 5b).

3.6 Microcomputed tomography analysis

The μ CT was used for tracking the new bone formation within the defects after surgery (Fig. 5c). Group M possessed better



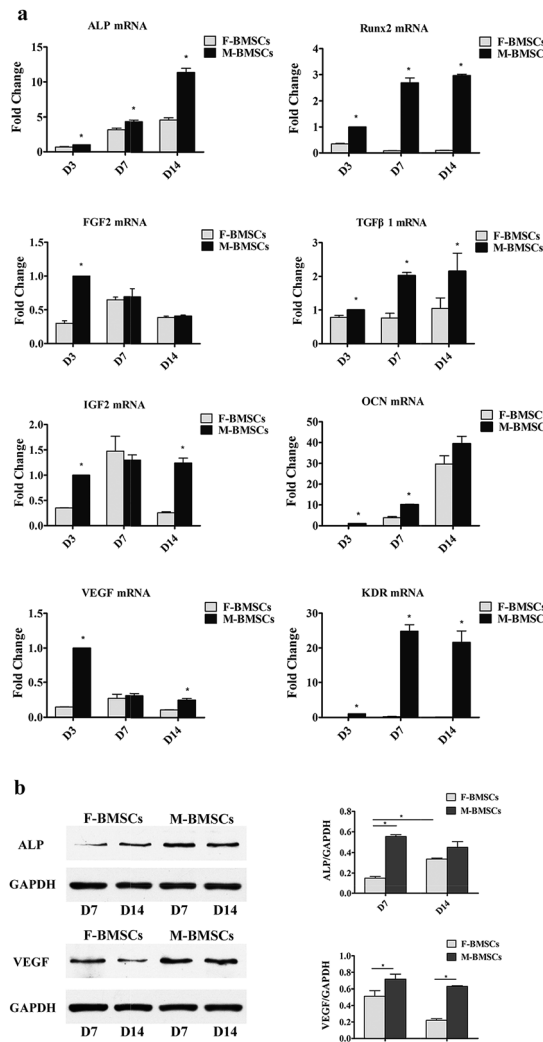


Fig. 3 (a) The osteogenic and angiogenic gene expression analysis: osteogenic genes of ALP, Runx2, FGF2, TGF β 1, IGF2 and OCN and angiogenic genes of VEGF and KDR expressions. (b) Western blotting analysis for ALP and VEGF protein expressions. * $p < 0.05$ indicates statistical significance between M-BMSCs group and the F-BMSCs group.

bone regeneration capacity compared with other three groups. Group F took the next place, while the group B showed the minimum bone formation was accompanied with periodontal bone loss. From the value of the bone mineral density (BMD) for each group, it seems that group M had significantly higher BMD compared with group F (Fig. 5d).

3.7 Morphological and immunohistochemical analysis *in vivo*

HE staining was used to observe new bone formation for surgical bone defect (Fig. 6a and b). The HE staining images showed that alveolar bone crests were replaced by growth of connective tissues. In addition new vascular structure appeared in four groups. Apparent new bone formation could be found in group F and group M, and the relative new bone area was larger in group M. Positive ALP and VEGF immunoreactivities were

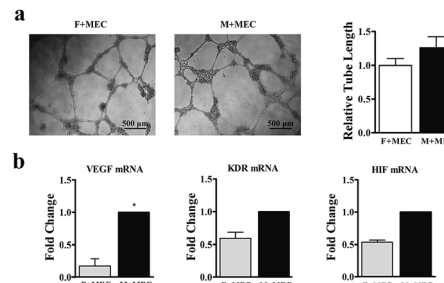


Fig. 4 (a) Tube formation assay and quantitative analysis of tube length. (b) Relative gene expression of MEC after co-culture with M-BMSCs and F-BMSCs * $p < 0.05$ indicates statistical significance between M + MEC group and the F + MEC group.

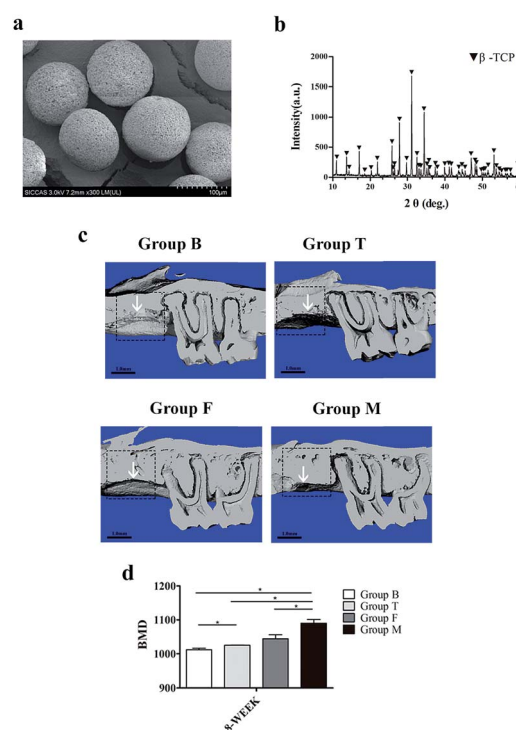


Fig. 5 (a) SEM micrograph and (b) XRD patterns of the β -TCP microspheres. (c) Microcomputed tomography analysis for the reconstructed images of the four groups: group B; group T; group F; group M. (d) Bone histomorphometric analysis for bone mineral density. * $p < 0.05$ indicates statistical significance between the groups; the white arrow indicates the bone regeneration endpoint.

detected in the four groups (Fig. 6c and d). From immunohistochemical analysis, it seems that group M still had active osteogenesis with higher ALP expression, while the group B contains more connective tissue with higher VEGF expression. The expression of ALP and VEGF between group F and group M had statistical significance.

4 Discussion

BMSCs contain the abilities to proliferate and differentiate into multi-lineage cells.³⁴ Transplantation of BMSCs promotes new

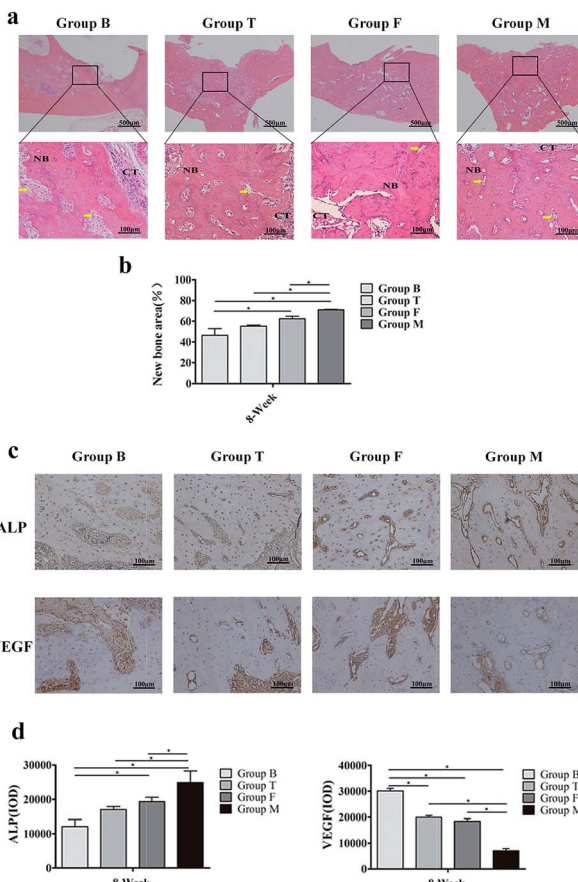


Fig. 6 Morphological and immunohistochemical analysis of the extraction sites. (a) HE staining for low magnification and high magnification images with newly formed bone (NB), connective tissues (CT), the yellow arrows indicate the vascular tissue. (b) Quantification of new bone area at 8 weeks after tooth extraction. (c and d) Immunohistochemical analysis of ALP and VEGF expression. $*p < 0.05$ indicates statistical significance between the groups.

bone regeneration and is commonly used as seed cells in bone regeneration and bone tissue engineering applications. Unlike stromal cells from the limb bone, maxillofacial bone marrow derived cells have site-specific characters. The developmental and clinical difference between F-BMSCs and M-BMSCs implies different bone formation potential. Previous studies have shown that craniofacial BMSCs had superiority over BMSCs from the limb bone. However, most of these studies focus on cells osteogenesis capacity of *in vitro*. Along with osteogenic capability, BMSCs also secret VEGF in a differentiation dependent manner during osteogenesis.³⁵

Osteogenesis and vascularization are two important stages in bone tissue regeneration. Vasculature, which precedes bone formation, supplies osteoblast necessary nutrients and can regulate activity of osteoblasts.^{20,34} Meanwhile, the proliferation and differentiation of osteoblasts promote bone matrix deposition, leading to the formation of new bone tissues. As the candidate seed cells for bone formation, both of F-BMSCs and M-BMSCs contain osteogenesis and angiogenesis potentials. As far as we know, without research has been performed to systematically compare osteogenic and angiogenic capabilities

between F-BMSCs and M-BMSCs. In order to choose the ideal seed cell sources, we studied and compared their cellular and histologic processes *in vitro* and *in vivo*.

In the present study, SPF level female SD rats of paired weight from the same family were used. Cells used in our *in vitro* and *in vivo* studies were also collected from the same SD rats. In the experiment procedure, we successfully isolated and cultured BMSCs from jaw bone and limb bone, respectively. The high purity of the cells was confirmed through flow cytometric analysis. BMSCs contain positive surface antigens, such as CD166, CD105, CD90, CD44, CD29 and CD13. CD79, CD45 and CD34 which were expressed in hematopoietic stem cells as well as bone marrow fibroblastic cells were negative in BMSCs.^{23,36} The different antigen levels might suggest they came from different sites.

Both of the two kinds of BMSCs contained stem cell state. Without significant morphology difference was observed between them until the 6th generation. F-BMSCs showed flat polygonal morphology at 6th generation. The CCK-8 assay also indicated lower proliferation rate in F-BMSCs at 6th generation. It revealed that M-BMSCs kept longer proliferation and different abilities when compared with F-BMSCs.^{37,38}

In order to compare the osteogenic potential between F-BMSCs and M-BMSCs, the two BMSCs were cultured in the same osteoblast inducing medium to detect the determination of ALP activity and calcium deposition. As the early maker of osteogenic differentiation, ALP hydrolyze the pyrophosphate which promotes the bone mineralization, and promotes the formation of apatite,³⁹ whereas calcium deposition marked the late stage of osteogenesis. We found that M-BMSCs had stronger ALP activity in the early stage of osteogenesis. The number of calcium node in M-BMSCs group was more than that in F-BMSCs group. It suggested that M-BMSCs contain better osteogenic potential. As a member of the stem cell family, BMSCs contains multipotent differentiation abilities. From the Oil Red O staining, F-BMSCs contained better adipogenic differentiation abilities.

Bone formation-related gene expressions including ALP, Runx2, FGF2, TGF β 1, IGF2 and OCN were further quantified by RT-PCR. In the present study, M-BMSCs showed significantly increased ALP, Runx2, FGF2, TGF β 1, IGF2 and OCN expression. Runx2 stimulates bone formation and osteoblast differentiation. FGF2 activates Runx2 by phosphorylation through Ras/MAPK/ERK pathway.⁴⁰ And TGF- β 1 and IGF2 enhances the proliferation of mesenchymal cells and osteoblasts in fractures as well as in experimental bone defects.⁴¹ As the most abundant collagenous protein in extracellular matrix, OCN involves in the later stages of osteogenesis and mineral formation.⁴² Compared with F-BMSCs, our *in vitro* study showed M-BMSCs with higher expression of these osteogenic factors entered into the later stage of bone formation earlier than F-BMSCs.

Under osteogenic induction condition, we found angiogenic factors including VEGF and KDR were expressed in the BMSCs. VEGF is a critical regulator in angiogenesis, and plays a significant role in skeletal growth. Previous studies had demonstrated that BMSCs tend to reside in perivascular and affect endothelial cells with growth factors and cytokines in a paracrine fashion.⁴³



As the receptor of VEGF, KDR has strong tyrosine kinase activity and is the main receptor to activate various signaling pathways.⁴⁴ The present study suggested that M-BMSCs and F-BMSCs promote vascularization along with bone formation. Higher expression of VEGF and KDR indicated better angiogenic potential for M-BMSCs. Moreover, the tube formation assay also confirmed that M-BMSCs promoted better angiogenesis compared to F-BMSCs. The result was further confirmed by VEGF and ALP on protein levels.

In order to further evaluate the osteogenic and angiogenic potential between F-BMSCs and M-BMSCs in bone defect regeneration applications, the BMSCs loaded β -TCP microspheres were implanted into the defect. The β -TCP microspheres with a higher specific surface area might play a suitable carrier to deliver the cells, and they are also suitable for cellular infiltration and proliferation.⁵ The results from μ CT assay indicated that β -TCP contained ability to promote bone regeneration *in vivo*. It seems that the β -TCP microspheres has been absorbed after 8 weeks of the surgery.⁴⁵ However, bone regeneration ability was more active in the groups loaded with BMSCs as seed cells. The mean BMD was significantly higher in M-BMSCs group compared with F-BMSCs group and β -TCP group. To further confirm this, histologic examination was performed. From HE staining and immunohistochemical analysis, the percentage of new bone area and the ALP expression were statistically higher in M-BMSCs group. It seems that M-BMSCs as seed cells have better capability to accelerate the bone healing *in vivo*, and the result was in consistent with the studies *in vitro*.

In addition, the development and formation of new bone is accompanied with vascular ingrowth. The vessel in connective tissue provides necessary factors, such as growth factors, cytokines, and chemokines for bone marrow. Along with bone defect healing process, the connective tissue was gradually replaced by new bone.⁴⁶ From HE staining analysis, it seems that blood vessel in connective tissue decreased in BMSCs groups. The immunohistochemical analysis of VEGF expression also confirmed this tendency, as VEGF was only highly expressed during the early phase of bone defects regeneration.⁴⁷ It seems that M-BMSCs group is in a more mature stage of bone regeneration after 8 weeks of the surgery.

Taken together, the *in vivo* study proves that M-BMSCs contains better osteogenic and angiogenic capability as seed cells in mandibular bone regeneration and bone tissue engineering applications. However, whether the osteogenic potential of M-BMSCs is still better when applied for the restoration of any other site bone defects should be further investigated in details.

5 Conclusions

Seed cells serve as the important part in bone tissue engineering for clinic applications. The present studies demonstrated that M-BMSCs presents better osteogenic capability and higher secretion level of angiogenic factors than F-BMSCs in the same culture medium, and contained better bone regeneration capacity as seed cells in the process of maxillary defect

restoration. The results enhanced our understanding of seed cells, and helped us to choose the ideal seed cells for patients with maxillary bone defect and to develop new approaches for therapy.

Conflicts of interest

There are no conflicts to declare.

Acknowledgements

The authors gratefully acknowledge the support of the Natural Science Foundation of China (No. 81672134, 81371129, 81670973), Science and Technology Commission of Shanghai Municipality (No. 15441905300, 17510710800), and the Fund of Shanghai Municipal Commission of Health and Family Planning (grant No. 201540369).

Notes and references

- 1 L. Zhao, J. Li, L. Zhang, Y. Wang, J. Wang, B. Gu, J. Chen, T. Hao, C. Wang and N. Wen, *RSC Adv.*, 2016, **6**, 62071–62082.
- 2 Y. Yu, S. Hua, M. Yang, Z. Fu, S. Teng, K. Niu, Q. Zhao and C. Yi, *RSC Adv.*, 2016, **6**, 110557–110565.
- 3 N. Cui, J. Qian, J. Wang, Y. Wang, W. Xu and H. Wang, *RSC Adv.*, 2016, **6**, 97096–97106.
- 4 J. Mitra, G. Tripathi, A. Sharma and B. Basu, *RSC Adv.*, 2013, **3**, 11073.
- 5 J. Jia, W. Siheng, C. Fang, A. Chengchong and C. Shiyi, *RSC Adv.*, 2016, **6**, 41800–41808.
- 6 J. M. Seong, B. C. Kim, J. H. Park, I. K. Kwon, A. Mantalaris and Y. S. Hwang, *Biomed. Mater.*, 2010, **5**, 535–547.
- 7 M. Tatullo, M. Marrelli and F. Paduano, *Int. J. Med. Sci.*, 2014, **12**, 72–77.
- 8 K. Lin, L. Xia, H. Li, X. Jiang, H. Pan, Y. Xu, W. W. Lu, Z. Zhang and J. Chang, *Biomaterials*, 2013, **34**, 10028–10042.
- 9 Y. Xiao, S. Mareddy and R. Crawford, *Int. J. Oral Sci.*, 2010, **02**, 127–135.
- 10 H. Ohnishi, Y. Oda and H. Ohgushi, *Sci. Technol. Adv. Mater.*, 2010, **11**, 014110.
- 11 C. Seebach, D. Henrich, A. Schaible, B. Relja, M. Jugold, H. Bönig and I. Marzi, *Tissue Eng., Part A*, 2015, **21**, 1565–1578.
- 12 Y. Xu, Z. Wu, X. Dong and H. Li, *RSC Adv.*, 2017, **7**, 5306–5314.
- 13 A. J. Gaggl, H. K. Burger and F. M. Chiari, *Br. J. Oral Maxillofac. Surg.*, 2008, **46**, 211–217.
- 14 A. Gaggl, H. Bürger, S. Virnik, P. Schachner and F. Chiari, *Cleft Palate Craniofac. J.*, 2012, **49**, 305–313.
- 15 Y. Ichikawa, J. Watahiki, T. Nampo, K. Nose, G. Yamamoto, T. Irie, K. Mishima and K. Maki, *J. Periodontal Res.*, 2015, **50**, 468–478.
- 16 A. Abzhanov, S. J. Rodda, A. P. McMahon and C. J. Tabin, *Development*, 2007, **134**, 3133–3144.





17 T. L. Aghaloo, T. Chaichanasakul, O. Bezougliaia, B. Kang, R. Franco, S. M. Dry, E. Atti and S. Tetradiis, *J. Dent. Res.*, 2010, **89**, 1293–1298.

18 S. O. Akintoye, P. Giavis, D. Stefanik, L. Levin and F. K. Mante, *Clin. Oral Implants Res.*, 2008, **19**, 1197–1201.

19 W. Dong, J. Ge, P. Zhang, Y. Fu, Z. Zhang, J. Cheng and H. Jiang, *Cell Tissue Res.*, 2014, **358**, 165–175.

20 J. M. Kanczler and R. O. C. Oreffo, *Eur. Cells Mater.*, 2008, **15**, 100–114.

21 Y. Du, F. Jiang, Y. Liang, Y. Wang, W. Zhou, Y. Pan, M. Xue, Y. Peng, H. Yuan, N. Chen and H. Jiang, *J. Mol. Histol.*, 2016, **47**, 153–168.

22 A. Smajilagić, M. Aljičević, A. Redžić, S. Filipović and A. Lagumđžija, *Bosnian J. Basic Med. Sci.*, 2013, **13**, 27.

23 M. F. Pittenger, A. M. Mackay, S. C. Beck, R. K. Jaiswal, R. Douglas, J. D. Mosca, M. A. Moorman, D. W. Simonetti, S. Craig and D. R. Marshak, *Science*, 1999, **284**, 143–147.

24 X. Xing, K. Cheng, W. Cheng, T. Zhou, J. Min and J. Xu, *J. Pharm. Biomed. Anal.*, 2016, **129**, 466–472.

25 A. J. Rahyussalim, J. A. Pawitan, A. R. Kusnadi and T. Kurniawati, *Medical Journal of Indonesia*, 2016, **25**, 10.

26 M. M. Bradford, *Anal. Biochem.*, 2015, **72**, 248–254.

27 J. Baharara, E. Amini, M. A. Kerachian and M. Soltani, *Iran. J. Basic Med. Sci.*, 2014, **17**, 626–631.

28 Y. Zhou, Y. Wu, X. Jiang, X. Zhang, L. Xia, K. Lin and Y. Xu, *PLoS One*, 2015, **10**, 172–174.

29 A. Zaminy, K. I. Ragerdi, M. Barbarestani, A. Hedayatpour, R. Mahmoudi and N. A. Farzaneh, *Iran. Biomed. J.*, 2008, **12**, 133.

30 J. Fafínlabora, P. Fernándezpernas, I. Fuentes, T. J. De, N. Oreiro, S. Sangiaoalvarellos, J. Mateos and M. C. Arufe, *Sci. Rep.*, 2015, **5**, 16765.

31 K. Lin, J. Chang, J. Lu, W. Wu and Y. Zeng, *Ceram. Int.*, 2007, **33**, 979–985.

32 K. Lin, L. Chen, H. Qu, J. Lu and J. Chang, *Ceram. Int.*, 2011, **37**, 2397–2403.

33 X. Gong, W. Yu, H. Zhao, J. Su and Q. Sheng, *Sci. Rep.*, 2017, **7**, 36129.

34 R. A. Carano and E. H. Filvaroff, *Drug Discovery Today*, 2003, **8**, 980–989.

35 H. Mayer, H. Bertram, W. Lindenmaier, T. Korff, H. Weber and H. Weich, *J. Cell. Biochem.*, 2005, **95**, 827–839.

36 R. J. Deans and A. B. Moseley, *Exp. Hematol.*, 2000, **28**, 875–884.

37 S. F. H. D. Witte, E. E. Lambert, A. Merino, T. Strini, H. J. C. W. Douben, L. O'Flynn, S. J. Elliman, A. J. E. M. M. d. Klein, P. N. Newsome and C. C. Baan, *Cytotherapy*, 2017, **19**, 798–807.

38 M. Dhanasekaran, S. Indumathi, R. P. Lissa, R. Harikrishnan, J. S. Rajkumar and D. Sudarsanam, *Cytotechnology*, 2013, **65**, 187.

39 U. Sharma, D. Pal and R. Prasad, *Indian J. Clin. Biochem.*, 2014, **29**, 269–278.

40 K. Y. Choi, H. J. Kim, M. H. Lee, T. G. Kwon, H. D. Nah, T. Furuichi, T. Komori, S. H. Nam, Y. J. Kim and H. J. Kim, *Dev. Dyn.*, 2005, **233**, 115.

41 L. S. Beck, E. P. Amento, Y. Xu, L. Deguzman, W. P. Lee, T. Nguyen and N. A. Gillett, *J. Bone Miner. Res.*, 1993, **8**, 753.

42 J. H. Lee, J. H. Park, A. El-Fiqi, J. H. Kim, Y. R. Yun, J. H. Jang, C. M. Han, E. J. Lee and H. W. Kim, *Acta Biomater.*, 2014, **10**, 2750–2761.

43 M. Gnechchi, Z. Zhang, A. Ni and V. J. Dzau, *Circ. Res.*, 2008, **103**, 1204–1219.

44 L. Claesson-Welsh, *Biochem. Soc. Trans.*, 2011, **437**, 169–183.

45 F. Monchau, A. Lefèvre, M. Descamps, A. Belquinmyrdycz, P. Laffargue and H. F. Hildebrand, *Biomol. Eng.*, 2002, **19**, 143–152.

46 K. Tatsuyama, Y. Maezawa, H. Baba, Y. Imamura and M. Fukuda, *Eur. J. Histochem.*, 2000, **44**, 269–278.

47 S. Ohtsubo, M. Matsuda and M. Takekawa, *Histol. Histopathol.*, 2003, **18**, 153–163.